









## Effect of angulation of 3D printed resin provisional bridges: an *in vitro* study on hardness and fracture loading

Efeito da angulação de pontes provisórias de resina impressa em 3D: um estudo *in vitro* sobre a dureza e carregamento à fratura

Laís Maria de Barros BATISTA<sup>1</sup> , Yan Victor Silva de SANTANA<sup>2</sup> , Maria Terêza Lopes de Moura BORBA<sup>1</sup> ,  
Tayná Karla Arruda e SILVA<sup>1</sup> , Clarisse Maria Luiz SILVA<sup>2</sup> , Antonio José TÔRRES NETO<sup>2</sup> , Larissa Araújo Lopes BARRETO<sup>2</sup> ,  
Viviane Maria Gonçalves de FIGUEIREDO<sup>3</sup> 

1 - Universidade Federal de Pernambuco, Recife, PE, Brazil.

2 - Universidade do Estado de São Paulo, Instituto de Ciência e Tecnologia, Departamento de Materiais Odontológicos e Prótese, São José dos Campos, SP, Brazil.

3 - Universidade Federal de Pernambuco, Departamento de Prótese e Cirurgia Oral e Facial, Recife, PE, Brazil.

**How to cite:** Batista LMB, Santana YVS, Borba MTL, Silva TKA, Silva CML, Torres Neto AJ, Barreto LAL, Figueiredo VMG. Effect of angulation of 3D printed resin provisional bridges: an *in vitro* study on hardness and fracture loading. Braz Dent Sci. 2025;28(1):e4581. <https://doi.org/10.4322/bds.2025.e4581>

### ABSTRACT

**Objective:** to evaluate the effect of printing angle of three-dimensional (3D) printed resin temporary bridges, through an *in vitro* study on hardness and fracture loading. **Material and Methods:** Specimens fixed bridges with three elements (N=5) and block specimens (N=1), were distributed among the experimental groups based on different printing angles: 0°, 45°, and 90°. Surface analysis using a scanning electron microscope (SEM) was conducted on one specimen from each experimental group. Hardness testing was then performed, with the specimens receiving five measurements on a Vickers microhardness tester and for fracture loading testing, force was applied using a piston attached to a testing machine. Finally, the bridge specimens were evaluated for fracture. Fracture loading and hardness data were subjected to a Anova 1 Factor statistical test ( $p < 0.05$ ), while the findings from surface analysis and fractures were analyzed qualitatively. **Results:** On the surfaces of the specimens, printing layers were mainly observed in the 90° group for block-type specimens. For hardness analysis, the 3D printing angle showed statistical significance between groups ( $P = 0.000$ ), while no significant difference was found for fracture loading ( $P = 0.177$ ). Finally, there was a prevalence of all failures for the 0° and 90° groups and retainer fracture for the 45° group. **Conclusion:** Different angles of provisional bridges manufactured by 3D printed resin affect hardness, but do not interfere with fracture loading.

### KEYWORDS

Angulation; Dental prosthesis; Digital technology; Provisional bridges; Three-dimensional printing.

### RESUMO

**Objetivo:** avaliar o efeito da angulação de impressão das pontes provisórias de resina impressa tridimensional (3D), através de um estudo *in vitro* sobre dureza e resistência à fratura. **Material e Métodos:** Espécimes pontes fixas de 03 elementos (N=5) e espécimes em bloco (N=1) foram distribuídos entre os grupos experimentais quanto às diferentes angulações de impressão, 0°, 45°, 90°. Análise superficial em microscópio eletrônico de varredura (MEV) foi realizada em ambos tipos de espécimes (N=1). No teste de dureza, os espécimes receberam 05 medições em microdurômetro Vickers e no teste de carregamento à fratura, a força foi aplicada através de um pistão fixado a uma máquina de ensaio. Por fim, os espécimes em forma de ponte foram avaliados quanto à fratura. Os dados de carregamento à fratura e dureza foram submetidos ao teste estatístico Anova 1 Fator ( $p < 0.05$ ), os achados da análise superficial e fratura foram analisados qualitativamente. **Resultados:** Nas superfícies dos espécimes, as camadas de impressão são observadas principalmente no grupo 90° em espécime tipo bloco. Para a análise de dureza, a angulação da impressão 3D foi estatisticamente significativa entre grupos

( $P=0.000$ ), enquanto para o carregamento à fratura não foi identificada diferença entre grupos ( $P=0.177$ ). Houve prevalência de todas as falhas para os grupos  $0^\circ$  e  $90^\circ$  e fratura de retentor para o grupo  $45^\circ$ . **Conclusão:** Diferentes angulações de pontes provisórias fabricadas por uma resina impressa 3D promovem impacto sobre a dureza, contudo não interferem no carregamento à fratura.

## PALAVRAS-CHAVE

Angulação; Prótese dentária; Tecnologia digital; Pontes provisórias; Impressão tridimensional.

## INTRODUCTION

Provisional prostheses must be made from materials capable of withstanding the changes in the oral environment and occlusal forces for a certain period, especially in cases of oral rehabilitation lasting months or implant-supported prostheses [1,2]. In the search for long-lasting provisional alternatives, the fabrication of such prostheses using Computer-Aided Design – Computer-Aided Manufacturing (CAD/CAM) technology has become more popular, straightforward, and accessible in dental practice [1,3,4]. Studies such as those by Myagmar et al. [5] and Al-Qahtani et al. [6] indicate that three-dimensional (3D) printed provisional resins are suitable as temporary restorative materials for extended clinical use. Additionally, research by Pereira et al. [7] highlights the dimensional accuracy achievable with 3D-printed provisional crowns, which is crucial for ensuring stability and fit in long-term temporary restorations.

Polymer-based materials are widely used to produce dental crowns using additive technology. However, studies evaluating the use of 3D printed materials in Dentistry in terms of their surface and mechanical properties, including flexural strength, surface roughness, hardness, and aesthetics, remain limited [7,8]. Several factors are still not established for 3D printed provisional resins, such as the type of printer, printing parameters, layer thickness, and post-processing, which are crucial for understanding their impact on mechanical properties and the failure of printed restorations [9,10].

Studies have shown that print orientation is a factor that seems to influence the mechanical properties of 3D printed resins due to the distinct polymerization of layers during the printing process [9,11,12,13]. Thus, this printing parameter presents a gap in the literature, and building scientific evidence will help improve

the quality of dental restorations and their performance in daily practice [7,9,11].

Based on the above, the objective was to evaluate the effect of the orientation of 3D printed resin provisional bridges through an *in vitro* study on hardness and fracture loading. The hypothesis tested was: Null Hypothesis - There will be no statistically significant difference regarding the orientation of 3D printed resin provisional bridges in relation to hardness and fracture loading.

## MATERIAL AND METHODS

### Specimen fabrication

In this study, two types of specimens were produced: fixed bridges with 3 units for mechanical fracture testing and blocks for hardness testing. Both specimens were also used for surface analysis.

For the fixed bridge with 3 units, a model with metal cylindrical abutments simulating a pontic for element 25 and abutments for elements 24 and 26 was created with the following parameters: the conical cylindrical abutments with a  $6^\circ$  taper had a height of 5.4 mm, with widths of 6.0 mm (premolar) and 7.4 mm (molar), and a cervical finish with a chamfer of 0.8 mm thickness [10]. The occlusal thickness of the bridge was 1.5 mm, the circular connector had a dimension of 16.0 mm<sup>2</sup>, and the distance from the base of the connector to the model was 7 mm [11].

The metal preparations were scanned with a bench scanner to reproduce the design in CAD. This generated a Standard Tessellation Language (STL) file, which was transferred to a dental design software (exocad DentalCAD 2.2 Valetta; exocad GmbH) to design the fixed bridge, which had a cement space of 0.08 mm [1,10]. Meanwhile, the blocks measuring 25 X 12 X 2 mm were designed using the same dental design software mentioned earlier. (Figure 1)

### 3D printing

The STL file for the specimens was processed using slicing software (Photon Workshop, version V2.1.21; Anycubic, Shenzhen, China). The specimens were then printed using a 3D printer (Anycubic Photon S Talmax Dental Prosthesis Printer, Curitiba, Paraná, Brazil) using the Digital Light Processing (DLP) method. The printing of the provisional resin specimens (Resin Bio Prov; Prizma 3D Makertech Labs, Brazil - composition: Acrylate and Triacrylate Monomers Proprietary, Amorphous Silica, Fillers, Meta-Acrylate Oligomers, Diphenyl (2,4,6-trimethylbenzoyl)) was carried out at print angles of 0°, 45°, and 90° with a layer thickness of 0.05 mm, followed by a cleaning and curing process. After printing, the specimens were cleaned in isopropyl alcohol for 10 minutes using an ultrasonic bath and post-cured in a UV chamber for 10 minutes, according to the manufacturer's recommendations. Supports were removed using a bench motor and diamond disc cutter. Finally, the fit of the specimens on the metal preparations was verified. (Figure 1)

### Experimental groups

The experimental groups were defined by the printing angle (Table I). The sample size for this study was calculated using the Minitab statistical software (version 17 for Windows, Pennsylvania, USA), based on the standard deviation (27.8) from a similar study by Turksayar et al. [10] for fracture loading, resulting in an N=05 with a sample power of 80.0% concerning maximum differences. For hardness testing, 05 indentations were indicated for each block, according to a similar study by Crenn et al. [2]. Surface analysis in the study was performed with N=01, representing one specimen of each type per experimental group.

### Surface analysis

A significant sample from each experimental group with each type of specimen (N=1) was evaluated using Scanning Electron Microscopy (SEM) (HITACHI, Model TM300) to identify defects, pores, and the surface behavior of the material under study.

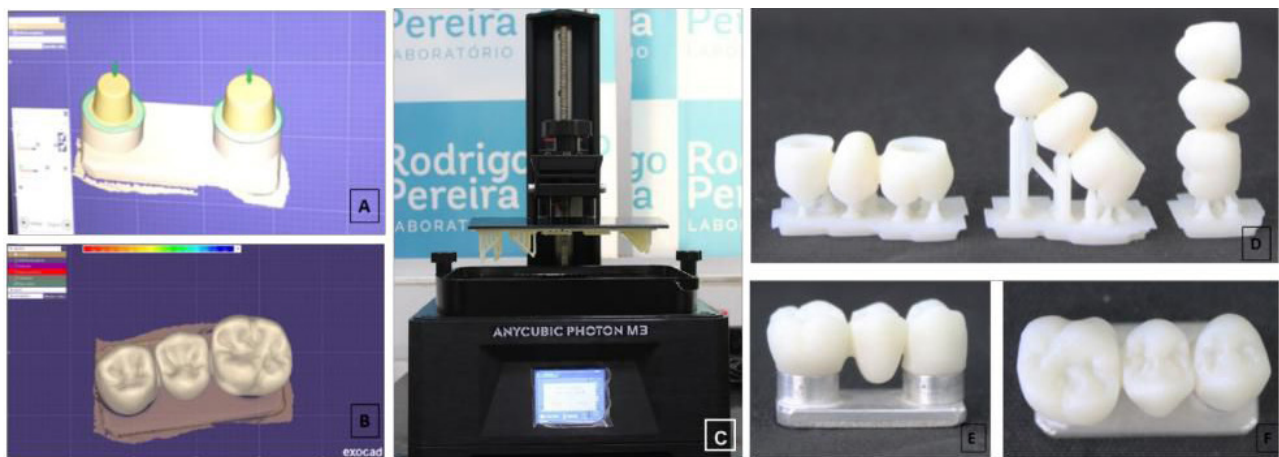


**Figure 1** - A and B - CAD planning; C - DLP printer; D - different printing angles of the provisional bridges, respectively 0°, 45° and 90°; E and F - bridges positioned on the metal preparation.

**Table I** - Description of the experimental groups and N sample of the study

Experimental Group	Description	N sample Block for Surface Analysis	N sample Fixed Bridge for Surface Analysis	N sample Fixed Bridge	N sample Indentations for Hardness (n=block)
0°	0° for printing angulation	N=1	N=1	N=5	N=5 (n=1)
45°	45° for printing angulation	N=1	N=1	N=5	N=5 (n=1)
90°	90° for printing angulation	N=1	N=1	N=5	N=5 (n=1)



## Hardness

Block specimens underwent 05 measurements using a Vickers microhardness tester (Micromet 5101, Buehler), under a load of 500 g and a dwell time of 20 seconds [2]. Five indentations were made on each specimen near the center, with at least 0.5 mm spacing. The major diameters of the Vickers indentations (d1 and d2) were measured with an optical micrometer, and hardness was calculated using Formula 1:

$$\text{Hardness} = \frac{1850 \times \text{load}}{(d1 \times d2)} \quad (1)$$

Formula 1: hardness calculation.

## Fracture loading test

To measure the fracture force, a compression test was conducted on the fixed bridge. The force was applied perpendicularly to the central fossa of the second premolar at a speed of 1 mm/min using a piston with a 4 mm diameter stainless steel sphere fixed to a testing machine (Emic DL-1000, Emic, São José dos Pinhais, PR, Brazil) [10]. Maximum fracture values were obtained in Newtons (N) for each group. No cementation of the bridges on the metal preparations was performed for the test. Additionally, during the test, a 0.5 mm thick aluminum foil was placed between the pontic and the piston to avoid peak forces [11].

## Fracture analysis

The fractured specimens were analyzed to determine the characteristics of the fractures. Failures were categorized based on fractures in the connector area, pontic, and retainer, presence

of cracks, and all failures occurring together, following the study by Turksayar et al. [10].

## Statistical analysis

Results were tabulated and analyzed using Minitab (version 17 for Windows, Pennsylvania, USA), with a significance level of 5%. The data for fracture loading and hardness were evaluated for the effect of printing angle using a 1-Factor ANOVA test ( $p < 0.05$ ). When differences between experimental groups were identified, the Tukey test ( $p < 0.05$ ) was applied to the study data. The Kolmogorov-Smirnov test was performed to determine the normality of the data, which was observed for hardness ( $p > 0.150$ ) and fracture loading ( $p > 0.150$ ). Surface and fractographic analyses were evaluated qualitatively.

## RESULTS

Based on the analyses conducted, it is observed that the surfaces of the specimens with different printing angles exhibit distinct morphologies, highlighting the characteristics of the printing layers, especially in the 90° angle group in the block-type specimen (Figure 2). Regarding hardness analysis, the 3D printing angle was statistically significant among groups ( $P = 0.000$ ), showing differences across all groups. The hardness values, in descending order, were highest at the 90° angle, followed by the 45° and 0° angles (Table II, Figures 3 and 4). From the perspective of surface analysis of the 3D printed bridges, a frequency of defects was observed on the buccal, occlusal, and palatal surfaces in the 0° and 45° groups, attributed to the presence of printing supports in these areas (Figures 5 and 6). There

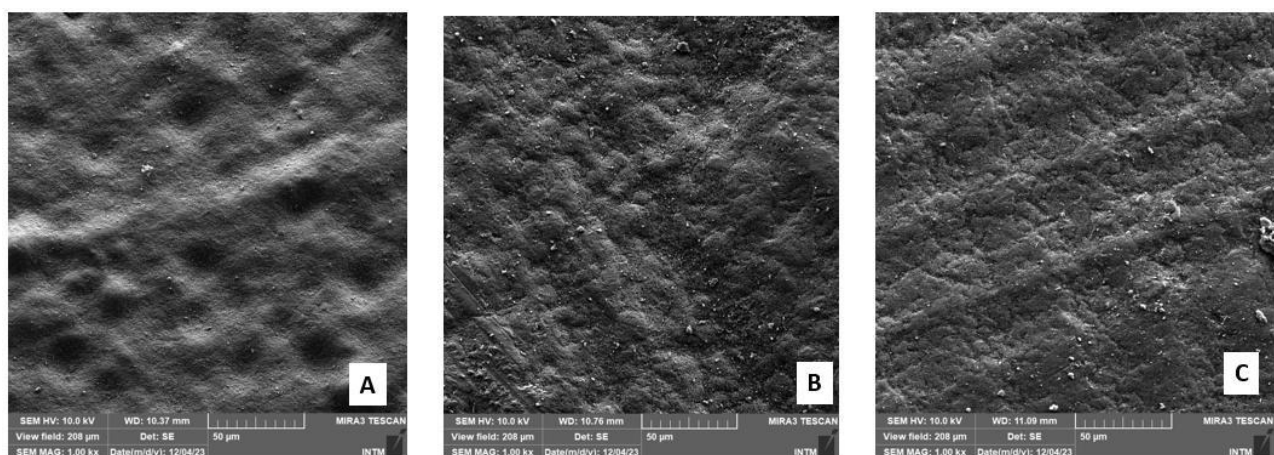


**Figure 2** - Scanning Electron Microscopy images at 1000X magnification, A - 0°; B - 45°; C - 90°.

Experimental Groups	Mean	Standard Deviation	Minimum	Maximum	P-value	Difference Between Groups**
0°	13.34	0.865	12.50	14.30	0.000	C
45°	17.56	1.401	16.25	19.20		B
90°	19.50	1.111	18.45	20.70		A

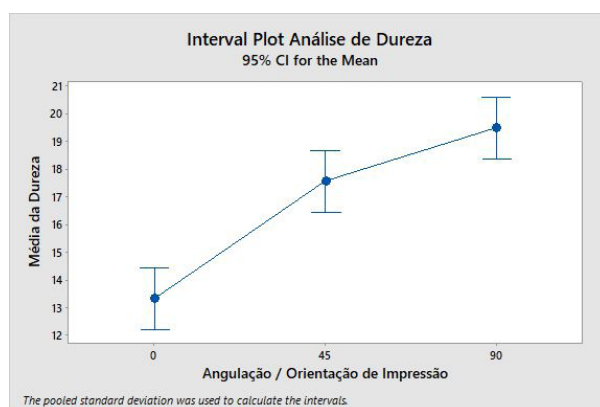
**Table III - Fracture Loading Data\***

Experimental Groups	Mean	Standard Deviation	Minimum	Maximum	P-value	Difference Between Groups**
0°	1101.9	178.1	887.8	1354.2	0.177	A
45°	850.0	334	256.0	1046.0		A
90°	1182.0	284	689.0	1413.0		A

Figure 1 consists of three scanning electron micrographs (A, B, and C) showing the surface morphology of the 3D-printed scaffolds. Each panel includes a 50 µm scale bar and technical data at the bottom.

- Panel A:** Shows a porous, interconnected network of struts. Technical data: 10.41 kV X1.00k 50µm, Diagonal: 1.296.3 µm, Diagonal: 1.237.7 µm, Diagonal: 1.171 µm.
- Panel B:** Shows a similar porous structure with a central circular feature. Technical data: 10.41 kV X1.00k 50µm, Diagonal: 1.296.3 µm, Diagonal: 1.237.7 µm, Diagonal: 1.171 µm.
- Panel C:** Shows a more complex, multi-layered porous structure. Technical data: 10.41 kV X1.00k 50µm, Diagonal: 1.296.3 µm, Diagonal: 1.237.7 µm, Diagonal: 1.171 µm.

was also a possible printing defect in the 0° group resulting in the presence of cracks (Figure 5). In the 90° group, as the supports are located on the proximal surface, no damage was recorded on the provisional bridge on the aforementioned surfaces (Figure 7). The investigated surfaces of the provisional bridges are similar in terms of the arrangement of the printing layers; however, there is a superficial alteration depending on the anatomical feature to be printed. Notably, there is a thicker intermediate layer between the printing layers in the 45° group (Figure 6), while in other experimental groups, there is a continuity between the printing layers. The fracture loading test did not identify differences between experimental groups ( $P=0.177$ ), with the 90° angle group showing the highest average force supported before fracture, followed by the 0° and 45° groups (Table III, Figure 8). Additionally, all types of failures were prevalent in the 0° and 90° groups, with retainer fractures observed in the 45° group (Table IV, Figures 9, 10, and 11).



## DISCUSSION

Based on the data obtained from the research, the null hypothesis—that there would be no statistically significant difference concerning the angulation of 3D-printed resin provisional bridges in relation to hardness and fracture loading—

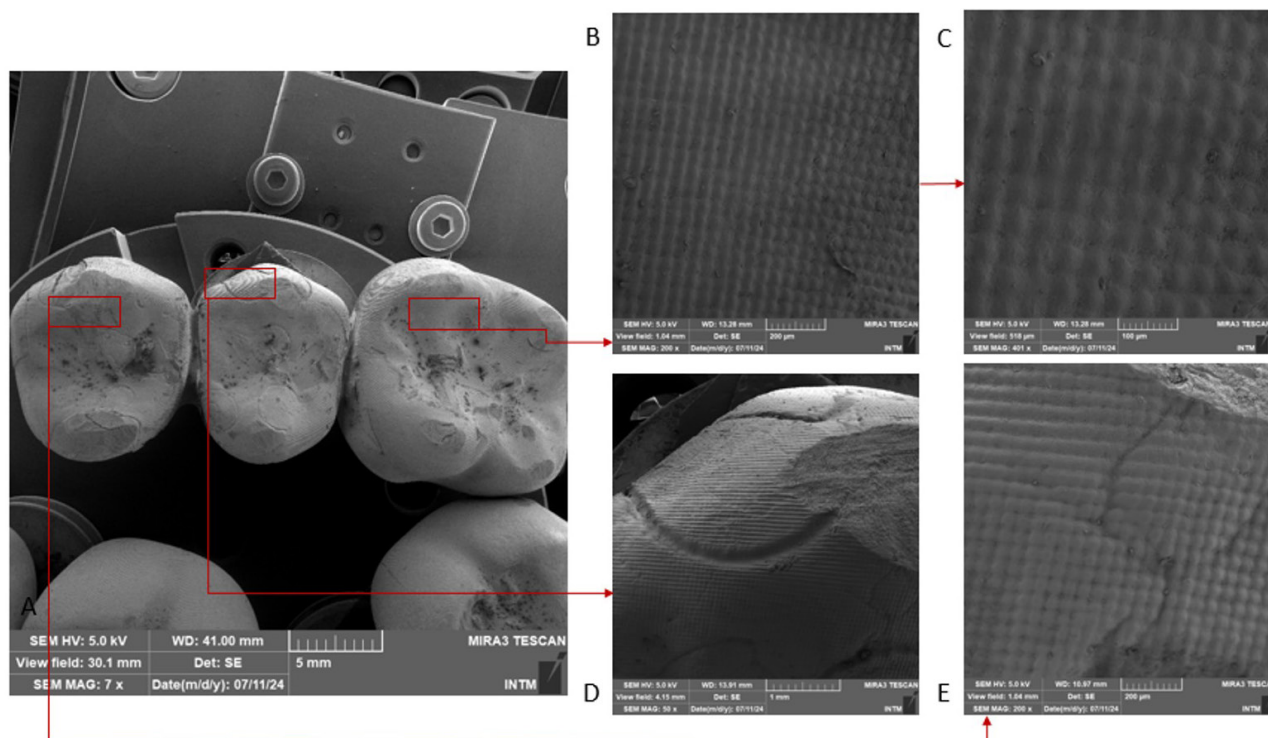


**Figure 5** - Group 0°, A - bridge with some defects due to support removal on the occlusal surface (6.9X magnification), B and C - occlusal surface of the first molar (200X and 400X magnification, respectively), D - second premolar with printing failures between the buccal and occlusal surfaces (50X magnification), and E - cracks and defects on the occlusal surface of the first premolar (200X magnification).

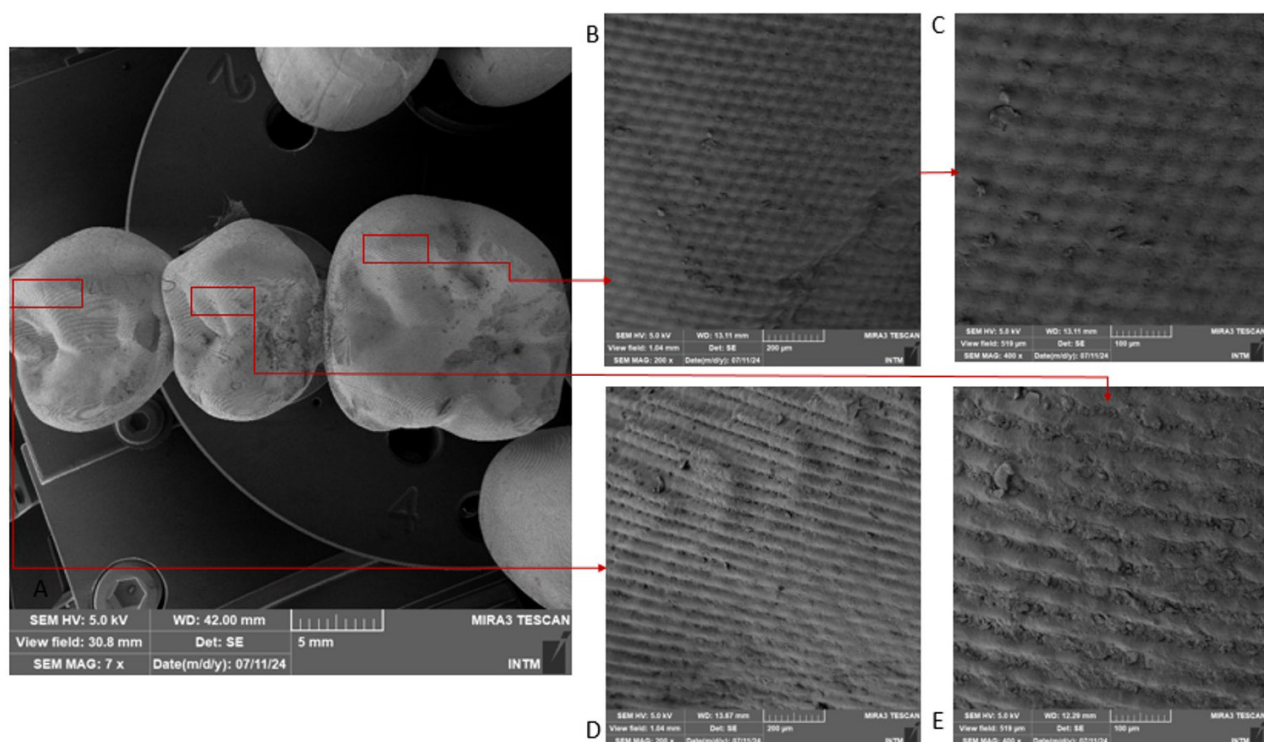


**Figure 6** - 45° group, A - bridge with some defects due to removal of the support on the occlusal surface (6.7X magnification), B and C - occlusal surface of the first molar (200X and 400X magnification, respectively), D - first premolar showing impression layers in the cusp region (200X magnification), and E - second premolar showing an intermediate layer between the impression layers (400X magnification).

was partially accepted. This is because the 3D printing angulation was statistically significant with respect to hardness.

Regarding the surface analysis, the distinct observation of printing layers in the specimens (geometric and anatomical) was also noted in



Table IV - Fracture Data

Experimental Group	Crack	Fracture Retainer	Fracture Pontic	Fracture Connector	All Failures
0°	01	01	-	01	02
45°	-	03	02	-	-
90°	-	-	-	01	04
Total	01	04	02	02	06

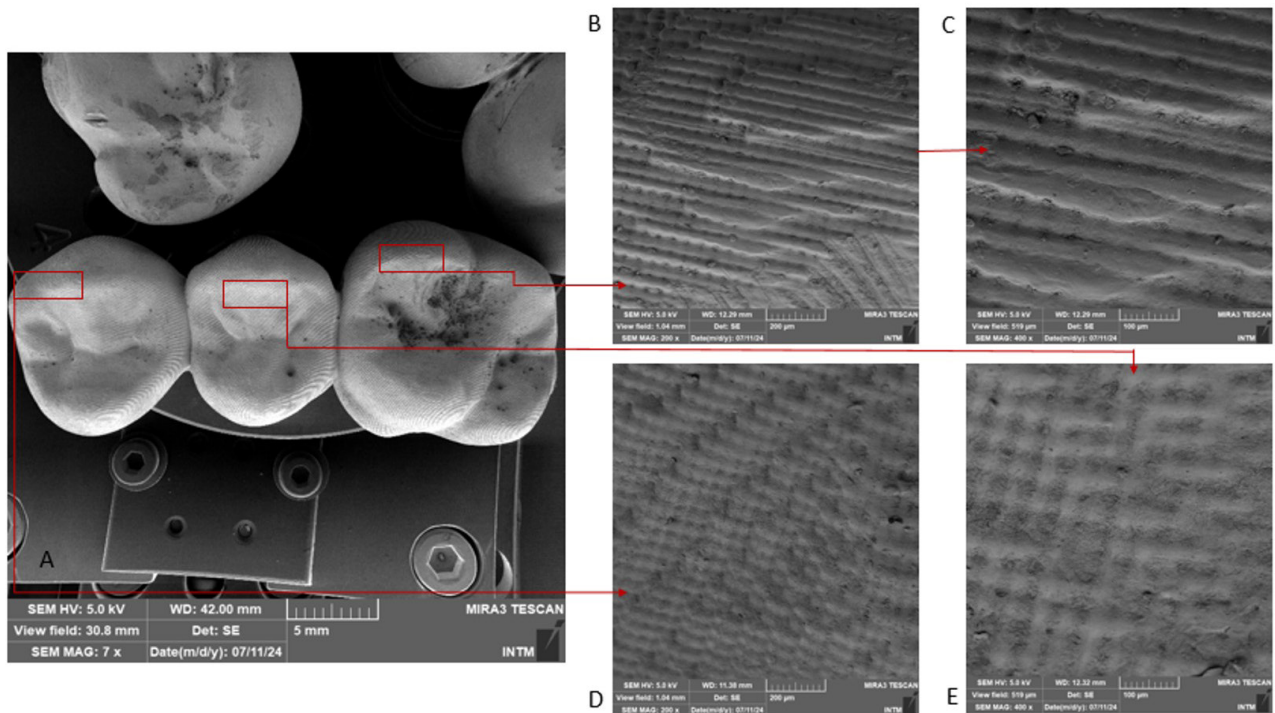


**Figure 7** - Group 90°, A - bridge without defects from support removal on the occlusal surface (6.7X magnification), B and C - mesio-buccal cusp of the first molar (200X and 400X magnification, respectively), D - first premolar showing printing layers on the buccal surface (200X magnification), and E - occlusal surface of the second premolar (400X magnification).

other studies, attributed to the DLP printing technique used in this research, where light is projected in pixel form onto the printing surface, polymerizing the resin layer by layer [3,8]. Another observation is that the surfaces of geometric and anatomical specimens showed distinct characteristics. When the specimens were blocks, a heterogeneous surface pattern was identified among the groups, with the printing layers being more evident at 90° compared to 0° and 45°, due to the adopted printing angulation.

The morphologies of these surfaces may also reflect a different roughness profile, though this was not measured in this study. Some studies comparing 3D-printed resin with conventional resin show varying results. For instance, Myagmar et al. [5] found that the 3D-printed resin group presented a

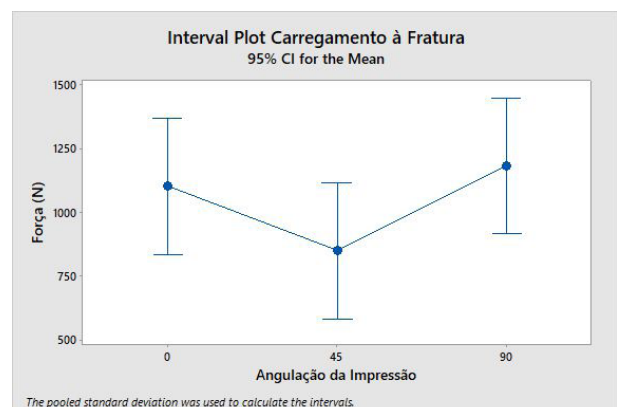


**Figure 8** - Experimental groups for the fracture loading test.

significantly smoother surface before and after aging compared to the conventional technique. Simoneti et al. [4] reported similar surface

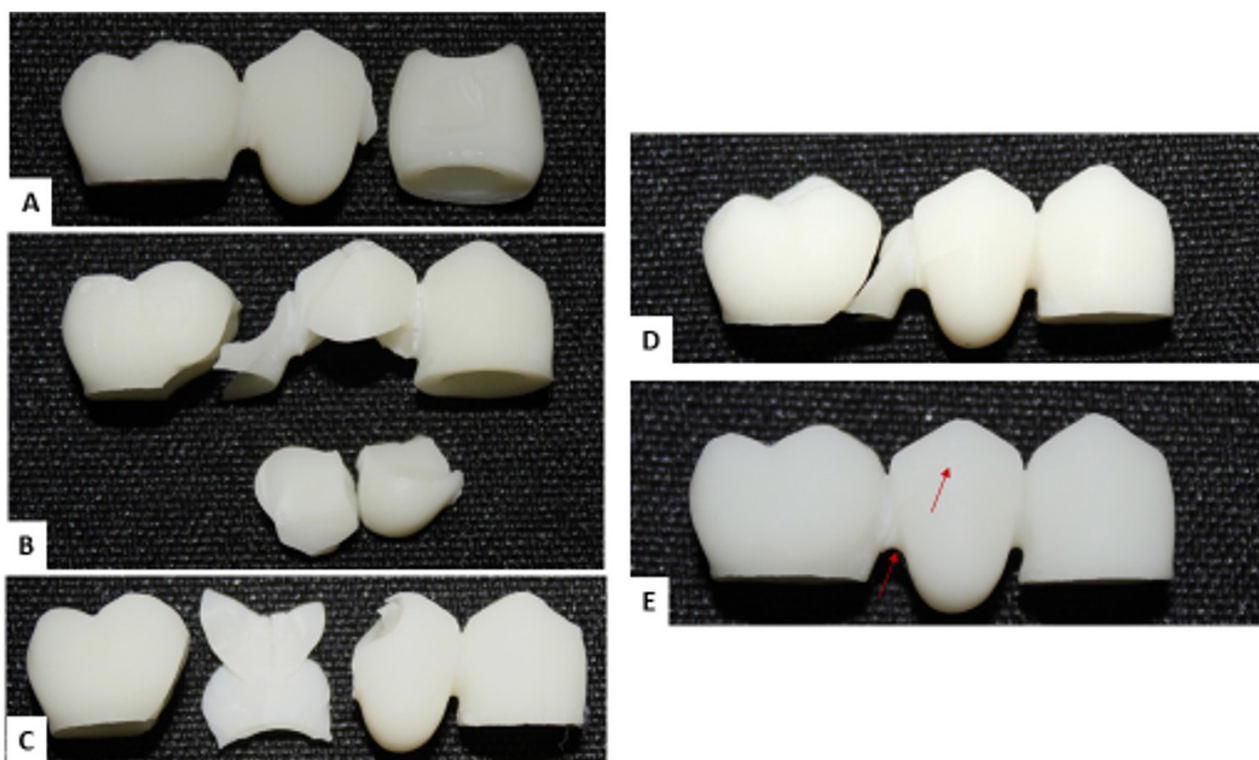


**Figure 9** - Experimental Group 0°; A - connector fracture, specimen 1; B and C - all failures, specimens 2 and 3, respectively; D - retainer fracture, specimen 4; E - crack in the connector and pontic region, specimen 5.

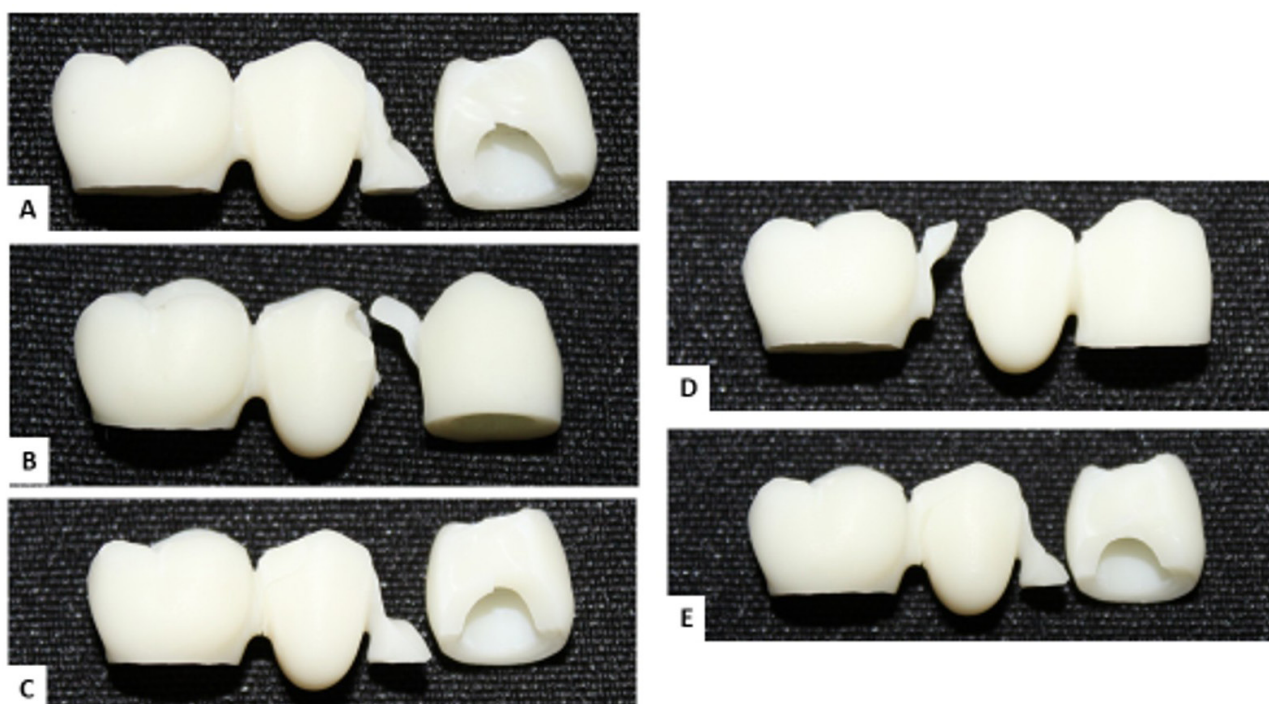


**Figure 10** - Experimental Group 45°; A - retainer fracture, specimen 1; B - pontic fracture, specimen 2; C - retainer fracture, specimen 3; D - pontic fracture, specimen 4; E - retainer fracture, specimen 5.

roughness data between 3D-printed specimens and those made using conventional methods. However, Al-Qahtani et al. [6] found higher

roughness in the 3D-printed sample group, which could be attributed to material composition or different printing angles across studies.



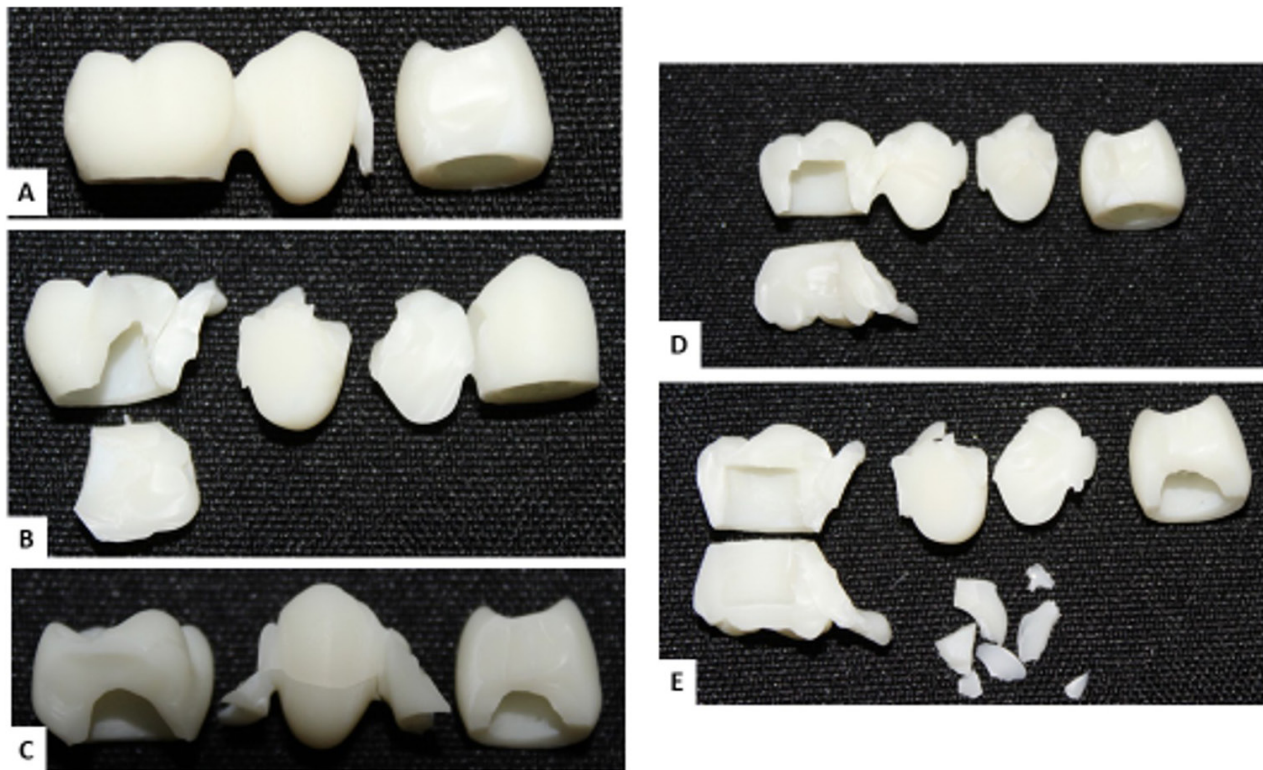


**Figure 11** - Experimental Group 90°; A - connector fracture, specimen 1; B, C, D, E - all failures, specimens 2, 3, 4, and 5, respectively.

For geometric specimens, the presence of various anatomical features might have caused the surfaces to appear more similar at 0°, 45°, and 90° angles. This surface condition might explain the lack of statistical difference between experimental groups after fracture loading. This is contrary to Park et al. [12], who suggested that the surface morphology of a 3D-printed object could be related to some mechanical properties, such as flexural strength and fracture resistance. However, that study compared different DLP printing techniques, stereolithography, and fused deposition modeling, and did not analyze angulation as a printing parameter.

Regarding the surface of the bridges, the presence of supports, especially on the occlusal face at 0° and 45°, led to the identification of several anatomical damages on the provisional bridge. In this study, no finishing or polishing of the specimens was performed; the tests were conducted immediately after printing and support removal. These defects need to be clinically addressed with finishing and polishing to prevent bacterial plaque accumulation, difficulty in occlusal adjustment, or potential patient harm. At 90°, since the supports are located on the proximal face, the provisional bridge's cementation process is facilitated

with fewer adjustments, reducing clinical time. Cracks identified at 0° might be due to the printing orientation, which may limit the formation of higher anatomical features like cusps. Additionally, the wide and rough bonding interface between printing layers at 45° is due to the printing technique. In DLP, each layer is formed from a single image displayed on the DMD chipset, and lines in each layer appear rough due to the chipset's resolution limit. In areas where layer bonding is weak, fractures may occur more quickly if the surface is rough [12]. This factor may explain the lower average fracture loading values in this experimental group.

In this study, printing angulation was a statistically significant factor for the hardness of this material, which is an important finding for the dental community. The analysis of this variable has not been previously observed in studies measuring the hardness of 3D-printed resins for crowns or provisional bridges. The literature indicates that the hardness of the resins studied can be affected by the printing technique [2], composition [2], printing layer [7], and may show different results compared to other types of provisional resins [4,6], with most studies not mentioning printing angulation in their methodology. Thus, hardness results may be explained by the testing condition.

Even if the specimen is printed in layers with a 90° orientation, the hardness test is conducted with the specimen in a horizontal position. This means that there is difficulty in indenting directly between printing layers in the 45° and 90° groups, thus promoting rupture between them. Therefore, the 0° group obtained a lower hardness value as the test was conducted on the specimen's surface without directly reaching the printing layers. A similar scenario was observed in Reymus et al. [11], where specimens in the distal position showed a higher fracture load compared to the occlusal position, due to greater resistance to layer separation in the direction of the mechanical test force.

No statistical difference was observed in fracture loading between the printing angles, contrary to studies by Reymus et al. [11] and Turksayar et al. [10]. Post-fracture data may be explained by the morphological similarity between specimens. According to Park et al. [12], the mechanical properties of 3D-printed resins reflect their morphological presentation. Various commercial resins exhibit different surface conditions regarding particle size, matrix, and dimension. Therefore, the morphology and chemical composition of the resin influence the mechanical properties of this temporary material [9]. Aging of specimens in Turksayar et al. [10] (thermomechanical with 120000 cycles and baths at 5 - 55°C) and Reymus et al. [11] (21 days of storage in distilled water at 37°C) may alter the thicker bonding layers, resulting in differences in fracture load values. Additionally, stereolithography's detail enhancement, which cannot be replicated with DLP, and the different chemical composition of the tested resin contributed to different results from the current research.

Regarding the fracture pattern, this study evaluated all specimens after achieving fracture, meaning the test was not stopped upon identifying the first crack. Thus, there was a higher frequency of all fractures occurring simultaneously in the specimen, resulting in multiple fragments. This result supports Park et al. [12] on the fracture of three-element bridges using the DLP technique, where the low elasticity of the tested resin generated multiple fragments, particularly in the connector area. It is worth noting that the increasing volume of these fragments may cause harm to the patient after fracture, due to the 3D-printed resin's composition based on acrylate

monomers, which has good surface hardness but is brittle due to its chemical structure. Moreover, the greater prevalence of all failures in the 0° and 90° groups can be explained by their ability to withstand higher loads until fracture, with greater layer compression and fewer surface damages, especially in the 90° group. This contrasts with the conditions observed in the 45° group regarding average fracture force and the intermediate layer between printing layers.

The limitations identified in this research included the lack of aging, comparison of other printing angles, and additional analyses. Further studies should investigate fracture loading after mechanical cycling, identify the origin of specimen fractures, and perform analyses of elastic modulus and fracture toughness to gather *in vitro* information for subsequent controlled clinical trials and validate the use of 3D-printed resins for provisional bridges in daily clinical practice.

## CONCLUSION

Based on the results obtained from this *in vitro* research, it was observed that different printing angles for provisional bridges manufactured with 3D-printed resin affect the hardness, but do not impact the fracture loading.

## Author's Contributions

LMBB: Methodology, Software, Writing - Original Draft, Formal Analysis, Investigation, Visualization. YVSS: Formal Analysis, Writing - Review & Editing. MTLMB: Formal Analysis, Writing - Review & Editing. TKAS: Formal Analysis, Writing - Review & Editing. CMLS: Formal Analysis, Writing - Review & Editing. AJTN: Formal Analysis, Investigation, Writing - Review & Editing, Visualization. LALB: Formal Analysis, Investigation, Writing - Review & Editing, Visualization. VMGF: Conceptualization, Methodology, Validation, Supervision, Project Administration.

## Conflict of Interest

No conflicts of interest declared concerning the publication on this article.

## Funding

The authors declare that no financial support was received.

## Regulatory Statement

None.

## REFERENCES

1. Reeponmaha T, Angwaravong O, Angwarawong T. Comparison of fracture strength after thermo-mechanical aging between provisional crowns made with CAD/CAM and conventional method. *J Adv Prosthodont*. 2020;12(4):218-24. <http://doi.org/10.4047/jap.2020.12.4.218>. PMID:32879712.
2. Crenn MJ, Rohman G, Fromentin O, Benoit A. Polylactic acid as a biocompatible polymer for three-dimensional printing of interim prosthesis: mechanical characterization. *Dent Mater J*. 2022;41(1):110-6. <http://doi.org/10.4012/dmj.2021-151>. PMID:34866117.
3. Berli C, Thieringer FM, Sharma N, Müller JA, Dedem P, Fischer J, et al. Comparing the mechanical properties of pressed, milled, and 3D-printed resins for occlusal devices. *J Prosthodont*. 2019;10.024. PMID:31955837.
4. Simoneti DM, Pereira-Cenci T, Santos BF. Comparison of material properties and biofilm formation in interim single crowns obtained by 3D printing and conventional methods. *J Prosthet Dent*. 2022;127(1):168-72. <http://doi.org/10.1016/j.prosdent.2020.06.026>. PMID:33168174.
5. Myagmar G, Lee JH, Ahn JS, Yeo SL, Yoon HI, Han JS. Wear of 3D printed and CAD/CAM milled interim resin materials after chewing simulation. *J Adv Prosthodont*. 2021;13(3):144-51. <http://doi.org/10.4047/jap.2021.13.3.144>. PMID:34234924.
6. Al-Qahtani AS, Tulbah HI, Binhasan M, Abbasi MS, Ahmed N, Shabib S, et al. Surface properties of polymer resins fabricated with subtractive and additive manufacturing techniques. *Polymers (Basel)*. 2021;13(23):4077. <http://doi.org/10.3390/polym13234077>. PMID:34883581.
7. Pereira ER, Sichi LGB, Coelho MS, Lopes GC, Araújo RM. Dimensional accuracy of provisional complete crown made by the 3D printing method. *Braz Dent Sci*. 2024;27(2):e4366. <http://doi.org/10.4322/bds.2024.e4366>.
8. Oliveira JR, Rodriguez LS, Finck NS. O fluxo de trabalho e a aplicação da impressão 3D na odontologia. *Revista Eletrônica Acervo Saúde*. 2023;23(5):e12747. <http://doi.org/10.25248/reas.e12747.2023>.
9. Kleber A, Hickel R, Ilie N. *In vitro* investigation of the influence of printing direction on the flexural strength, flexural modulus and fractographic analysis of 3D-printed temporary materials. *Dent Mater J*. 2021;40(3):641-9. <http://doi.org/10.4012/dmj.2020-147>. PMID:33456026.
10. Turksayar AA, Donmez MB, Olcay EO, Demirel M, Demir E. Effect of printing orientation on the fracture strength of additively manufactured 3-unit interim fixed dental prostheses after aging. *J Dent*. 2022;124:104155. <http://doi.org/10.1016/j.jdent.2022.104155>. PMID:35526752.
11. Reymus M, Fabritius R, Kleber A, Hickel R, Edelhoff D, Stawarczyk B. Fracture load of 3D-printed fixed dental prostheses compared with milled and conventionally fabricated ones: the impact of resin material, build direction, post-curing, and artificial aging—an *in vitro* study. *Clin Oral Investig*. 2020;24(2):701-10. <http://doi.org/10.1007/s00784-019-02952-7>. PMID:31127429.
12. Park SM, Park JM, Kim SK, Heo SJ, Koak JY. Flexural strength of 3D-printing resin materials for provisional fixed dental prostheses. *Materials (Basel)*. 2020;13(18):3970. <http://doi.org/10.3390/ma13183970>. PMID:32911702.
13. Alshamrani AA, Raju R, Ellakwa A. Effect of printing layer thickness and postprinting conditions on the flexural strength and hardness of a 3d-printed resin. *BioMed Res Int*. 2022;2022(1):8353137. <http://doi.org/10.1155/2022/8353137>. PMID:35237691.

**Antonio José Tôrres Neto**  
(Corresponding address)

Universidade do Estado de São Paulo, Instituto de Ciência e Tecnologia, São José dos Campos, SP, Brazil.  
Email: ajtn18@gmail.com

Date submitted: 2024 Nov 19  
Accept submission 2025 Mar 08